Human-in-the-Loop Weight Compensation and Mass Estimation in Upper Limb Wearable Robots Towards Muscles' Effort Minimization

Rezvan Nasiri[1*], Hamidreza Aftabi[1+] , Mojtaba Rayati, and Majid Nili Ahmadabadi[#]

***Abstract*— In this paper: (1) We present a novel human-in-the-loop adaptation method for whole arm muscles' effort minimization by means of weight compensation in the face of an object with unknown mass. (2) This adaptation rule can also be used as a cognitive model for the identification of mass value. (3) This adaptation rule utilizes the EMG signal of only four muscles in the upper limb to minimize the whole muscles' effort. The method is analyzed from analytical, simulation, and experimental perspectives. We analytically discuss the stability, optimality, and convergence of the proposed method. This method's effectiveness for whole muscles' effort reduction is studied by simulations (OpenSim) on a generic and realistic model of the human arm, a model with 7-DOF and 50 Hill-type-muscles. In addition, the applicability of this method in practice is experimented with by a 2-DOF arm assist device for two different tasks; static (holding an object) and cyclic (reaching point-to-point) tasks. The simulations and experimental results show the presented method's performance and applicability for weight compensation in upper limb assistive exoskeletons. In addition, the simulations in OpenSim completely support that the suggested set of mono-articular muscles are sufficient for whole muscles' effort reduction.**

***Index Terms*— Human-in-the-Loop, Weight Compensation, Mass Estimation, EMG Sensors, Upper Limb Exoskeleton**

I. Introduction

Despite of many efforts in design and control of upper limb wearable robots [1], [2], still, design of an effective control approach for upper limb assistance is a challenge; see [3-6]. And, many of the suggested methods for control of upper limb exoskeletons are not effective.

In classic control of exoskeleton systems, the human dynamics and torque were considered as external disturbances or uncertainties in which the controller tries to reject them. However, in human-robot-interaction or wearable robotic fields, the human is considered as a part of the control system such that the exoskeleton and human are collaborating with each to perform a certain task; i.e., human-in-the-loop [6-11]. To consider the human as a part of control strategy, several considerations should be met; the controller should: (1) minimize muscles' effort/force, (2) not impose a trajectory to the human, (3) utilize biofeedback, and (4) be adaptive.

An effective controller should provide the assistive torque profile and allow the human to have active voluntary behaviors instead of enforcing a predetermined reference trajectory; i.e., pure position control is inutile. There are several perspectives in the robotic field to address this property. For instance, in human-robot-interaction, the reference trajectories are adapted to the human's intended trajectory through interaction force minimization; see [12-14]. Although this is a very effective and applicable approach, it is mostly restricted to the cyclic or some specific motions; many upper limb human-exoskeleton tasks are noncyclic. In addition, the minimization of the interaction force does not necessarily lead to human muscles' effort/force reduction.

Another approach for upper limb assistance without imposing a reference trajectory is weight compensation, which is a task-independent (trajectory free) method; i.e., it is applicable for both cyclic and noncyclic tasks. Since the upper limb exoskeletons are mostly designed for picking, carrying, and placing heavy objects with slow dynamics, the gravitational torque is a high portion of required torque at each joint; i.e., weight compensation can reduce the muscle effort/force drastically. There are two different methods for weight compensation active and passive. The former generates the gravitational torque by actuators [15-18] and the later compensates the gravity effects with passive elements; e.g., spring or counterbalance [19-21]. However, most of the weight compensation exoskeletons are designed to generate a predefined torque profile; they are not useful for unknown object weight compensation. Besides, the human biomechanics has a time-varying nature even in repetitive tasks (e.g., walking) [22-24], which makes having an adaptive strategy to be a must [25].

There are many adaptive control approaches that update the exoskeleton torque based on the instantaneous feedback of the human body; see [6], [9], [26]. Among all possible biofeedback options, the electromyography signal is one of the best choices for torque adaptation due to its fast dynamics and monotonic relation with muscle force [27], [28]. Besides, EMG signals provide sufficient information for measuring muscle activity, force, fatigue, and metabolic rate; see [27], [29]. Accordingly, there are many works which benefit the EMG sensors for upper limb exoskeleton torque adaptation; e.g., see [4-6], [30-33]. Nevertheless, the proposed methods require the EMG signal of all contributing muscles which make them impractical, very complex, expensive, and time-costly; e.g., [30], [31] utilizes 16 EMG sensors. There are also some other works that utilized a smaller number of

[1] These authors contributed equally to this work
[*]Corresponding author; e-mail: nasiri.rezvan@gmail.com
[#]Principal corresponding author; e-mail: mnili@ut.ac.ir
[+] e-mail: hamidreza.aftabi@ut.ac.ir
All authors are with the Cognitive Systems Laboratory, Control and Intelligent Processing Center of Excellence (CIPCE), School of Electrical and Computer Engineering, College of Engineering, University of Tehran, Iran.

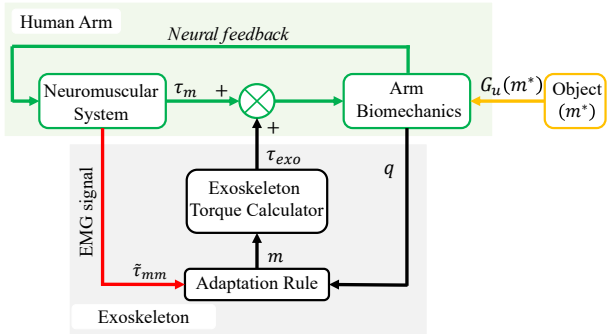

Fig. 1. The human-in-the-loop control block diagram: Human arm in interaction with an object with unknown mass (m^*) and weight compensation exoskeleton system; G_u is the gravitational effects of object. The adaptation rule utilizes the EMG signal of chosen muscles along with the joint positions to estimate mono-articular muscles' torque (τ_{mm}) and adapt m. The torque calculator block uses the adapted value of m to update the exoskeleton torque.

EMG sensors; see [4], [6], [32], [33]. However, these works are restricted to a single joint (mostly elbow), and they are basically designed for a specific task or device. In another perspective, they did not suggest a general and optimal adaptation rule with a minimum number of EMG sensors to achieve "muscles' total effort reduction."

Recently in [34], we presented the hypothesis that "feedback from mono-articular muscles is sufficient for exoskeleton torque adaptation and whole muscles' effort reduction". Benefiting from this hypothesis, we present a novel, simple, and effective weight compensation approach using a minimum number of EMG sensors, totally 4 EMG sensors for the whole arm. This generic adaptation method does not limit the users' voluntary motions, is task-independent (can be used for both cyclic and noncyclic tasks), and can be applied to different types of upper limb assistive devices for weight compensation. In addition, this adaptation rule provides us with a cognitive model to identify the object's mass value, which can be used as a model to describe human understanding about the environment by sensory information of muscles' force and joint positions.

II. Problem Statement

Consider the dynamical equations of the human-arm augmented by an upper-limb-exoskeleton (see Fig. 1) as:

$$M(q)\ddot{q} + C(q,\dot{q}) + G(q) + S(q,\dot{q}) = \tau_m + \tau_{exo} \quad (1)$$

where $q \in \mathbb{R}^n$ is the vector of the joints' positions, n is number of joints and m is the number of all contributing muscles. $\dot{q} \in \mathbb{R}^n$ and $\ddot{q} \in \mathbb{R}^n$ are first and second ordered time derivative of q. In addition, $M(.) : \mathbb{R}^n \to \mathbb{R}^{n\times n}$ is the mass matrix and $C(.) : \mathbb{R}^{n\times n} \to \mathbb{R}^n$ is the vector of Coriolis and Centrifugal force. $G(.) : \mathbb{R}^n \to \mathbb{R}^n$ is the vector of gravity force. And, $\tau_m \in \mathbb{R}^n$ is the muscles' net torque which is a summation of muscles' force; i.e., for jth joint we have $\tau_m^j = \sum_{i=1}^{m^j} f_i d_i(q,q')$ where $f_i \in \mathbb{R}^+$ and $d_i \in \mathbb{R}$ are ith muscles' force and lever arm[1], and m_j is the number of contributor muscles' at jth joint. Since muscles are either mono- or bi-articular d_i is a function of both targeted joint (q_j) and its adjacent joint q'_j positions. $S(.) : \mathbb{R}^{n\times n} \to \mathbb{R}^n$ is added to model dynamical effects of other biological elements; e.g., ligaments and tendons. Finally, $\tau_{exo} \in \mathbb{R}^n$ is the torque applied by exoskeleton[2].

Assuming that the human picks, carries, or places an object with unknown mass ($m^* \in \mathbb{R}^+$) and the exoskeleton is trying to compensate the effects of unknown mass by applying an external torque (τ_{exo}), the dynamical equations in Eq. 1 are rewritten as:

$$\underbrace{M^*(q)\ddot{q} + C^*(q,\dot{q}) + S^*(q,\dot{q})}_{MCS^*(q,\dot{q},\ddot{q})} + G^*(q) = \tau_m + \tau_{exo} \quad (2)$$

where M^*, C^*, G^*, S^* are parameters which are defined in Eq. 1 and affected by $m^* > 0$; if $m^* = 0 \to M^* \equiv M$, $C^* \equiv C$, $G^* \equiv G$, and $S^* \equiv S$. In this equation, G^* can be divided in two terms as $G^* = G + G_u$ where G is the gravity vector for $m^* = 0$ and G_u is the gravitational effects of m^*. G_u can be written as a function of position ($H(q)$) multiplied by m^*g as $G_u(q) = m^*gH(q)$, $H(.) : \mathbb{R}^n \to \mathbb{R}^n$ where $g = 9.81m/s^2$ is the gravity acceleration and $H(q)$ is a position dependent matrix. Hence, Eq. 2 is presented as:

$$MCS^*(q,\dot{q},\ddot{q}) + G(q) + m^*gH(q) = \tau_m + \tau_{exo}. \quad (3)$$

To compensate the gravity effect of an object, simply we can cancel out its dynamical effect by setting $\tau_{exo} = mgH(q) + \tilde{G}(q)$, where the first term is an adaptive term and, $m \in \mathbb{R}$ is left to adaptation, and $\tilde{G}(q)$ is the estimation of $G(q)$. In addition, $H(q)$ is defined based on the exoskeleton device; it is a predetermined function of position.

Henceforth, the problem is to present an adaptation method for m and updating the exoskeleton torque (τ_{exo}) to minimize the total muscles' effort. The total muscles' effort is defined as $J_t = \sum_{i=1}^{m}(f_i/f_{max})^2$ where f_{max} is the muscles' maximum isometric force [35]. Fig. 1 shows schematics for this adaptation method in which the adaptation rule block uses the EMG signal as biofeedback.

The adaptation of m for minimization of J_t does not necessarily converges to m^*. To **(1)** minimize J_t and **(2)** identify m^* at the same time by m adaptation, some certain conditions should be met. In the following section we discuss about this point with more details.

III. Mathematical Analysis

Whole of our mathematical analysis are presented without any assumption on the shape of the motions (cyclic or noncyclic) and the exoskeleton dynamics.

1) Optimality: As we proved in [34], the "whole muscles' effort" (J_t) reduction by exoskeleton torque optimization (τ_{exo}) is equivalent with the "squared of two antagonistic mono-articular muscles' torque" minimization (J_{mm}). In other words, the gradient of J_t w.r.t. the exoskeleton torque

[1] Since x is a vector in $\mathbb{R}^n$, x_j and x^j are both jth element of x.

[2] Note that in the rest of the paper, for the sake of simplicity and without loss of generality, we may forbear specifying the argument of the functions, e.g., $C(q,\dot{q})$ may represent C.

is in the same direction of the gradient of J_{mm} w.r.t. the exoskeleton torque; i.e., $\nabla_{\tau_{exo}} J_t \propto \nabla_{\tau_{exo}} J_{mm}$. Hence, to extract the adaptation, we use J_{mm} instead of J_t as:

$$J_{mm} = 0.5\tau_{mm}^T \tau_{mm} \tag{4}$$

where $\tau_{mm} \in \mathbb{R}^n$ is the torque vector of two antagonistic mono-articular muscles at each joint; for n joints, $2n$ mono-articular muscles are required. The muscle net torque can be rewritten as $\tau_m = \tau_{mm} + \tau_{bm} + \tau_{om}$, where $\tau_{bm} \in \mathbb{R}^n$ is the torque vector of bi-articular muscles and $\tau_{om} \in \mathbb{R}^n$ is the torque vector of remained mono-articular muscles; i.e., $\tau_{mm} = \tau_m - \tau_{bm} - \tau_{om}$.

2) Adaptation rule: To extract the adaptation rule, we apply the gradient descent on J_{mm} as $\dot{m} = -\lambda \tau_{mm}^T \partial \tau_{mm} / \partial m$. By substituting $\tau_{mm} = \tau_m - \tau_{bm} - \tau_{om}$, using Eq.3, replacing $\tau_{exo} = \tilde{G}(q) + mgH(q)$, we have the adaptation rule as:

$$\dot{m} = \epsilon \tau_{mm}^T H(q) = \epsilon H(q)^T \tau_{mm} \ , \ \epsilon = g\lambda \ , \ \epsilon > 0 \tag{5}$$

where ϵ is the adaptation rate which can control the adaptation performance; i.e., speed and accuracy of convergence. Using Eq.5 leads to instantaneous J_{mm}) minimization, and based on hypothesis presented in [34], consequently, minimization of J_{mm} leads to J_t reduction. Nevertheless, τ_{mm} cannot be directly computed, and in practice we estimate τ_{mm} using EMG signal of mono-articular muscles as $\tilde{\tau}_{mm} = \alpha_f d_f(q)\Gamma_f - \alpha_e d_e(q)\Gamma_e$ where α, $d(q)$, and Γ are tunning scale, muscle lever, and RMS EMG, respectively; see [34] and [36]. Besides, f and e indicates values related to flexor and extensor muscles. Due to imperfect estimation of τ_{mm}, we have $\tau_{mm} = \tilde{\tau}_{mm} + \tau_e$ where τ_e is error torque which is added to model imperfections of our estimation such that $\|\tau_{mm}\|_2 \gg \|\tau_e\|_2$.

3) Stability & convergence: To prove the stability and convergence of the adaptation rule (Eq. 5), we utilize $\tilde{\tau}_{mm}$ instead of τ_{mm} in the adaptation rule, replace τ_{mm} with $\tau_m - \tau_{bm} - \tau_{om}$, replace τ_m using Eq. 3, and rewrite the adaptation dynamics as:

$$\dot{m} = \epsilon H^T (MCS^* + G + m^* gH - \tau_{exo} - \tau_{bm} - \tau_{om} - \tau_e). \tag{6}$$

By substituting τ_{exo} with $\tau_{exo} = mgH + \tilde{G}$, we have:

$$\begin{aligned} \dot{m} &= -\epsilon g(m - m^*) H^T H + f(t) \ , \\ f(t) &= \epsilon H^T (MCS^* + G - \tilde{G} - \tau_{bm} - \tau_{om} - \tau_e). \end{aligned} \tag{7}$$

Theorem 1 (Stability & Convergence)**.** *The adaptation dynamics (Eq.7):*

1) *is stable.*
2) *is convergent towards m^* with error of δm, if (**C-1**) motions are sufficiently slow $(\dot{q}, \ddot{q}) \approxeq 0$.*
3) *is convergent towards m^*, if (**C-1**) motions are sufficiently slow $(\dot{q}, \ddot{q}) \approxeq 0$, and (**C-2**) $m^* \gg \|\Delta G\|_\infty + \|S^* - \tau_{bm} - \tau_{om} - \tau_e\|_\infty$.*

Proof. Stability proof: The dynamical equation in Eq. 7 is a summation of two terms **(1)** a globally asymptotically stable dynamics $(-\epsilon g(m - m^*) H^T H)$ with equilibrium of $m = m^*$ and **(2)** $f(t)$ which is a non-vanishing and bounded perturbation. Hence, based on [37, pp.346], the overall system is ultimately bounded and the adaptation dynamics (Eq.7) is stable. The stability of Eq.7 is proved without any assumption.

Convergence proof: If we assume that $(\dot{q}, \ddot{q}) \approxeq 0$ (**C-1**), consequently it is concluded that $M^* \ddot{q} + C^* \approxeq 0$. In this case, the adaptation dynamics is $\dot{m} = -\epsilon g(m - m^*) H^T H + \epsilon \beta$ where $\beta = H^T (S^* + \Delta G - \tau_{bm} - \tau_{om} - \tau_e)$ is almost a fixed function of time and $\Delta G = G - \tilde{G}$ is the gravity compensation error. Hence, the adaptation dynamics is rewritten as $\dot{m} = -\epsilon g(m - m^* - \delta m) H^T H$ where $\delta m = g^{-1} \beta (H^T H)^{-1}$ is mass convergence error.

If the dynamical effects of unknown mass is dominant to gravity compensation error (ΔG) and the dynamical effects of the biological elements $(S^* - \tau_{bm} - \tau_{om} - \tau_e)$ as $m^* \gg \|\delta m\|_\infty$ or $m^* \gg \|\Delta G\|_\infty + \|S^* - \tau_{bm} - \tau_{om} - \tau_e\|_\infty$ (**C-2**) the adaptation dynamics is $\dot{m} \approxeq -\epsilon g(m - m^*) H^T H$ which is convergent to m^*. If the conditions are not satisfied m converges to $m^\# = m^* + \delta m$. □

The adaptation rule is extracted to minimize J_{mm}; it is a gradient descent over J_{mm}. Hence, the equilibrium point of adaptation dynamics ($m^\#$) minimizes the J_{mm} and consequently based on [34] minimizes the total muscles' effort (J_t). However, $m^\#$ does not necessarily identify m^*; in general $m^\# \neq m^*$. Nevertheless, if **C-1** and **C-2** are satisfied, we can identify m^* along with J_t minimization. **C-2** indicates that $\Delta G \approxeq 0$; i.e., the exoskeleton weight should be known properly. In the following simulations and experiments, we study the performance of adaptation rule (Eq.5) on J_t reduction and the deviations of $m^\#$ from m^* in cases that **C-1** and **C-2** are violated.

IV. Simulation

In this section, using the OpenSim software [38], we study our adaptation rule's performance in three different tasks; in these tasks, we violate **C-1**. The musculoskeletal model utilized in this simulation is presented by Holzbaur *et al.* [39], which is a modified version of the previously released one [40]. This upper extremity model contains 7 degrees of freedom (shoulder 3-DOF, elbow 1-DOF, and wrist 3-DOF) and 50 Hill-type muscles introduced by Zajac *et al.* [41]. We scaled the generic model using the dataset presented in [39] to reach a model consistent with human anthropometry. To consider the unknown mass, a bucket with a mass of $5kg$ is attached to the model hand; see Fig.2a.

The task is to move the bucket on a circular trajectory in sagittal plane with radius of $12cm$ and three different frequencies; $\omega = 1rad/s$, $2rad/s$, and $4rad/s$. The main purpose of this task definition is to study the whole muscles' effort reduction and the equilibrium point of adaptation dynamics for **C-1** violation; $4rad/s$ is an extreme violation.

The designed exoskeleton in this model is two 1-DOF ideal actuators at the elbow and shoulder joints, which apply torque at the sagittal plane. The generated torque by the exoskeleton device is $\tau_{exo} = mgH(q) + \tilde{G}$ where $\tilde{G}$ is estimated gravity torque and m is adapted using Eq. 5, joints' position, the force signal (EMG) of four suggested

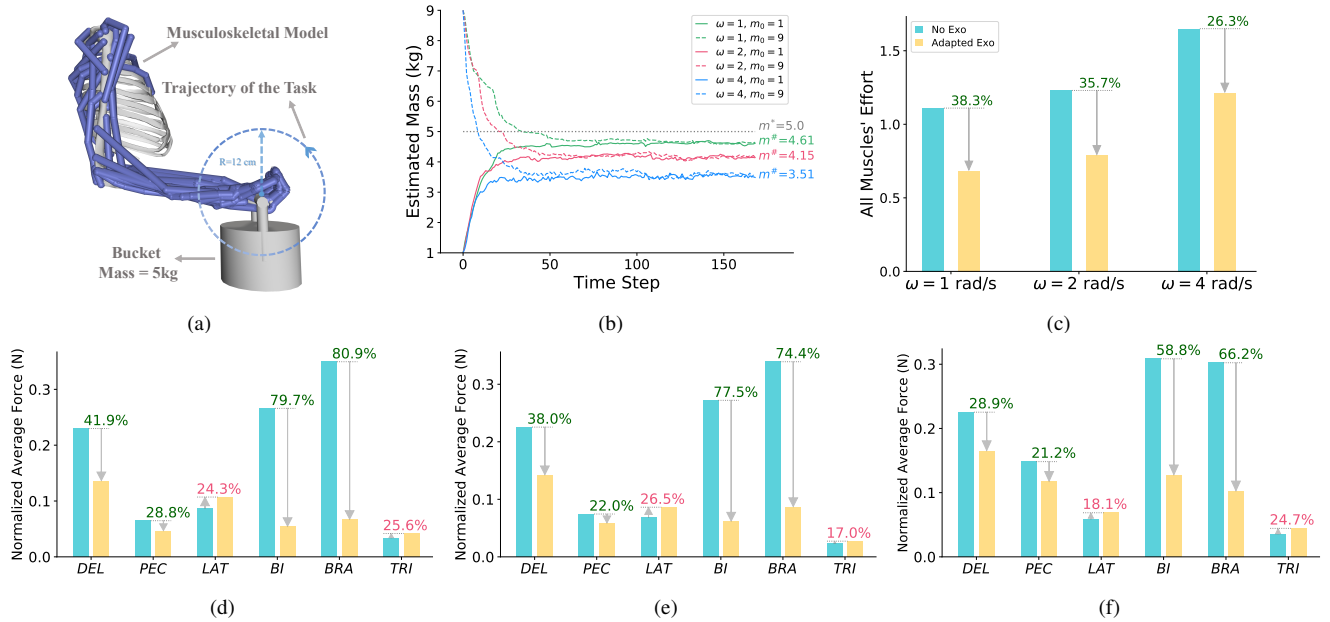

Fig. 2. (a) is the utilized biomechanical model in OpenSim for analyzing the behavior of adaptation in different conditions. The model consists of 7-DOF (shoulder 3-DOF, elbow 1-DOF, and wrist 3-DOF) and 50 Hill-type muscles. The task is to move the object with an unknown mass of $m^* = 5Kg$ over a circular trajectory with a radius of $12cm$ and three different frequencies $\omega = 1rad/s, 2rad/s, 4rad/s$. The exoskeleton consists of two 1-DOF ideal actuators that apply torque at shoulder and elbow joints in the sagittal plane. The goal is to compensate for the gravity effect of unknown mass at elbow and shoulder joints using force feedback (EMG signal) from four mono-articular muscles at elbow and shoulder joints. (b-f) are OpenSim simulation results for simultaneous mass identification and assistive torque adaptation. (b) show the adaptation performance for mass identification when the initial mass is set on $m_0 = 1Kg$ and $m_0 = 9Kg$, respectively. As it is clear, regardless of the initial point, the converged mass value is identical for each frequency. And, by increasing the frequency of motion, the converged mass value decreases from m^*. (c) shows the whole muscles' effort cost function (J_t) before and after adaptation. Clearly, the adaptation is successful for the the whole muscles' effort reduction. (d-f) compare the forces of six major muscles before and after adaptation in three different frequencies, respectively; Deltoid (DEL), Pectoralis major (PEC), Latissimus dorsi (LAT), Biceps (BI), Brachialis (BRA), and Triceps (TRI). Based on these figures, forces of the two muscles are increased. Note that reducing the main cost function (the average efforts of all muscles) does not necessarily mean each individual's effort reduction.

mono-articular muscles near to skin; Biceps and Triceps as antagonistic mono-articular muscles in elbow joint and Pectoralis major and Latissimus dorsi as antagonistic mono-articular muscles in shoulder joint. These muscles are also utilized for our experiments.

To simulate the adaptation performance, we run the OpenSim model within the MATLAB environment [42] where the input exoskeleton torques are updated based on Eq.5 in some certain intervals in MATLAB. In doing so, the simulation is chopped for 168 time steps in $37s$; each time interval is equal to $220ms$. In each time interval, the muscles' forces are calculated using the computed muscle control (CMC) algorithm [43] and based on the updated torques from the previous interval.

To study the convergence behavior of the adaptation for each frequency, the simulation is run from two different initial masses; $m_0 = 1Kg$ and $m_0 = 9Kg$. The results of this simulation are presented in Fig.2. Fig.2b shows the estimated mass value in the course of adaptation. Interestingly, the equilibrium point ($m^\#$) for each frequency is identical regardless of the initial point. Clearly, by moving from $\omega = 1rad/s$ to $\omega = 4rad/s$, the deviations of equilibrium point ($m^\#$) from $m^* = 5Kg$ increases with a linear pattern such that $\forall\omega \in [0\ 4] \rightarrow m^* \approxeq m^\# + 0.38\omega$ with estimation confidence of 95%.

Fig.2c-f describes the effect of m adaptation on total muscles' effort (J_t) and the force of six major muscles in the arm. Based on Fig.2c, regardless of the deviations of $m^\#$ from m^*, the adaptation of exoskeleton torque profile leads to total muscles' effort reduction, which provides strong support for our claim that adaptation of m based on feedback from four muscles leads to whole contributor muscles' effort minimization. In addition, it proves that the suggested set of mono-articular muscles are sufficient for upper limb exoskeleton torque adaptation. According to Fig.2d-e, four muscles have force reduction while two of them, which are extensor muscles, have force increment. This observation seems evident since flexor muscles are the main contributors in compensating the effect of gravity, and the adaptation rule is trying to minimize the total muscles' effort cost function, which does not necessarily lead to each individual muscles' force reduction.

V. Experimental Study

To study the adaptation performance and the applicability of the proposed method in practice, we apply this method on the 2-DOF assistive device presented in [34]. Nevertheless, due to the different purposes of this study compared to [34], the configuration of linear spring and the number of EMG sensors are different; see Fig. 3a. This device comprises of

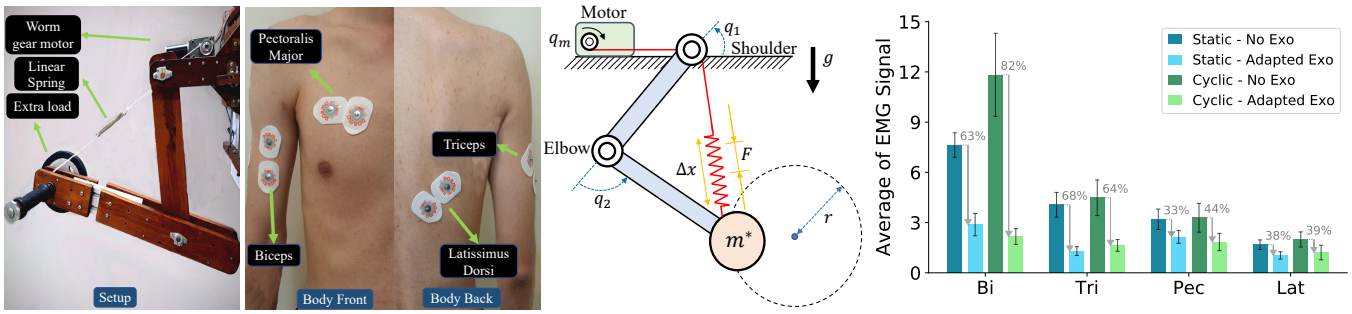

(a) (b) (c)

Fig. 3. (a) describes the experimental setup and the placement of the EMG electrodes. The assistive device is a wooden 2-DOF system with a linear spring and worm-geared motor for changing the spring displacement. In this setup, the potentiometers that measure the joints' positions are mounted on the other side of the setup and cannot be seen in this view. (b) shows the schematic of the aforementioned device. (c) compares the muscles' RMS EMG for $5s$ at the start of the adaptation with the last $5s$ of the adaptation process in static and cyclic tasks. The adaptation of weight compensation leads to EMG reduction in all muscles. The paired *t-test* results for static task are $P^*_{Bi} = 0.0035$, $P^*_{Tri} = 0.0299$, $P^*_{Pec} = 0.0383$, and $P^*_{Lat} = 0.0466$, and for cyclic task are $P^*_{Bi} = 0.0198$, $P^*_{Tri} = 0.0320$, $P^*_{Pec} = 0.0367$, and $P^*_{Lat} = 0.0029$.

two joints that their positions ($q \in \mathbb{R}^2$) are measured by potentiometers. In addition, it has a linear spring that applies torque to both shoulder and elbow joints. By using a worm gear motor, we can change the spring displacement and, consequently, the spring force. Hence, the effect of gravity can be compensated by controlling the position of the motor. The suggested set of muscles in the previous section are considered in this experiment as EMG sensory feedback; Biceps, Triceps, Pectoralis major, and Latissimus dorsi.

According to Fig.3b, in this experimental setup, the torque applied by the assistive device is $\tau_{exo} = J(q)F$ where $J \in \mathbb{R}^2$ is a transformation vector which is a function of position ($q \in \mathbb{R}^2$) and maps the linear spring force ($F \in \mathbb{R}$) into the torque ($\tau_{exo} \in \mathbb{R}^2$) at each joint. In this case, the linear spring force is $F = -k\Delta x$ where $k \in \mathbb{R}^+$ is the spring stiffness and $\Delta x \in \mathbb{R}$ is the spring displacement which is proportional to motor position $\Delta x = \rho q_m$; ρ is a proportional gain. By comparing $\tau_{exo} = Jk\rho q_m$ with $\tau_{exo} = mgH + \tilde{G}$, it is concluded that in this experimental setup, $\tilde{G} = 0$, $H = k\rho J$, and $m = q_m$; **C-2** is violated. Hence, based on Eq.5, the adaptation rule for controlling the motor position (q_m) is $\dot{q}_m = \mu J^T \tau_{mm}$, $\mu = k\rho\epsilon$ where μ is the adaptation rate. We utilize the suggested set of mono-articular muscles in Section IV to estimate τ_{mm}; Biceps, Triceps, Pectoralis major, and Latissimus dorsi.

Five healthy male subjects (age, 26 ± 1 years; mass, $78 \pm 12Kg$; height, $178 \pm 3cm$; mean±STEM) participated in this experiment. The purpose of this study was explained to the subjects. The subjects signed the informed consent forms and gave us the authority to use their information and test results. The committee at the University of Tehran has approved the experiment and the test protocol. Two different tasks are considered for this experiment; static and cyclic tasks. *Static task*: subjects hold the mass on a certain position similar to the position in Fig.3a. In this task, the muscles have isometric behavior. *Cyclic task*: subjects perform a cyclic "reaching-point-to-point" ([44]) task in the sagittal plane; see Fig. 3b. Subjects try to retain the desired frequency by hearing a recorded beep; $\omega = 4rad/s, r = 15cm$. In both tasks, the effective mass is equal to $m^* = 4Kg$, which is the exoskeleton's effective mass at the end-effector ($1.5Kg$) plus the mass of an unknown object ($2.5Kg$). The goal is to study EMG reduction, the convergence and the equilibrium point of the adaptation dynamics for the cases that **C-2** in static and **C-1** and **C-2** in the cyclic task are violated.

The results of this experiment are shown in Fig. 3c, Fig. 4, and Fig. 5. Fig. 3c provides an overall analysis for muscles' RMS EMG before and after adaptation. As can be seen, using the proposed adaptation rule leads to all muscles' EMG reduction. Compared to Section IV, not only flexors but also extensors' EMG signals are reduced, which is different from the simulation results in the previous section. A high portion of antagonistic muscles' co-activation force is the non-voluntary human neuromechanics behavior to ensure joint safety by increasing joint stiffness. Hence, compensation of a considerable amount of muscles' net torque by exoskeleton torque adaptation drastically reduces the required joint stiffness, which is the main source of antagonistic muscles' co-activation. In weight compensation of heavy objects, this behavior leads to both flexor and extensor muscles' effort reduction. This interesting behavior cannot be observed in OpenSim software since it cannot model antagonistic muscles' co-activation.

Fig. 4 shows the instantaneous behavior of the muscles' EMG signal in the course of adaptation. As it is clear, the adaptation of exoskeleton torque leads to a descending behavior in all muscles' EMG signals during the adaptation. Finally, Fig. 5 shows variations of m and converged equilibrium point ($m^{\#}$) in course of adaptations. Similar to our simulation results, here, by moving from static task ($\omega = 0rad/s$) to cyclic task ($\omega = 4rad/s$), $m^{\#}$ (the equilibrium point of adaptation dynamics) differs from $m^* = 4Kg$ drastically; i.e., for static and cyclic tasks $m^{\#}$ is $3.75Kg$ and $2.5Kg$, respectively.

We had a significant deviation from our theoretical assassinations in all experiments and even simulations ($\omega =$

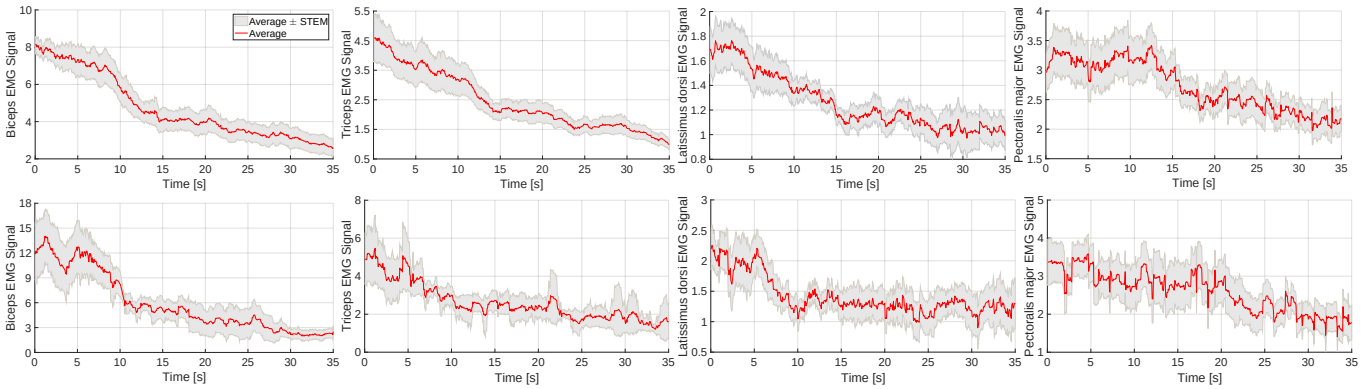

Fig. 4. Mean value and STEM for EMG signal of all muscles/tasks in the course of adaptation. The first row shows the instantaneous RMS EMG of 4 muscles for the static task. The second row shows the instantaneous RMS EMG of 4 muscles for the cyclic task. As can be seen, the Biceps and Triceps, the most contributor muscles in the defined tasks, achieve the maximum reduction. EMG signals of all muscles in both tasks show a reducing behavior. The RMS EMG is computed by a moving window of 500 samples (sampling rate is set to 250Hz).

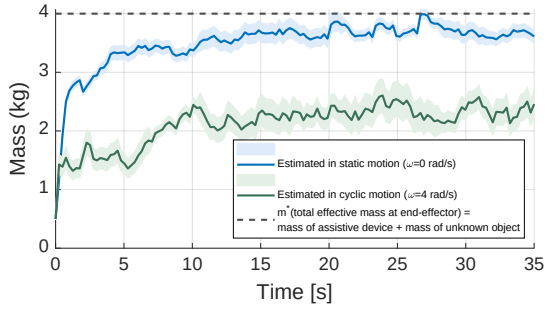

Fig. 5. The online performance of adaptation dynamics, which shows the smoothed m in course of adaptation. The initial m is set to $m_0 = 0.5Kg$. As it is clear, for both tasks, the adaptation dynamics is convergent while the equilibrium point for static task is $m^{\#} = 3.75Kg$ and for cyclic task is $m^{\#} = 2.5Kg$.

$2rad/s, 4rad/s$); however, the adaptation dynamics is stable, convergent, and optimal, which minimizes the muscles' EMG signal in the experiment and total muscles' effort in simulations. Note that in Section III, we have showed that the adaptation dynamics minimizes J_t instantaneously and is stable without any extra assumptions, and satisfying **C-1** and **C-2** is just for $m^{\#} \approxeq m^*$. Nevertheless, if the proposed method is going to be used for m^* identification, **C-1** and **C-2** should be satisfied properly.

VI. Conclusion and Discussions

In this paper, we presented a novel, simple, and effective human-in-the-loop approach for weight compensation in upper-limb assistive devices. This adaptation rule by feedback from four mono-articular muscles adapts the exoskeleton torque profile in order to compensate for the gravitational effects of the object with an unknown mass. Since the adaptation rule is defined for weight compensation, it is task-independent, does not enforce a certain trajectory to the human joints. Hence, the human can have active voluntary behaviors while a portion of the required torque at each joint is compensating by the exoskeleton device using the proposed adaptation rule. The presented method is also analyzed analytically in terms of optimality, stability, and convergence.

We suggested a set of four muscles for EMG signal measurement and accordingly exoskeleton torque profile adaptation, which leads to the whole muscles' effort reduction in the arm. Our simulation supports this claim on a generic and realistic model of the human arm in OpenSim, a model with 7-DOF and 50 Hill-type muscles. It is also observed that increasing the frequency/speed of the motions lead to a reduction in the estimation of unknown mass; i.e., deviations of equilibrium point from the unknown mass has a linear relation with frequency. The adaptation rule performance is also experimented in practice using a 2-DOF arm assistive device and the suggested set of mono-articular muscles in simulations. The experiment is done for two different (static and cyclic) tasks with five participates. It is observed that this adaptation rule leads to an EMG reduction in all of the muscles both for cyclic ad static tasks.

In this paper, we presented a model for mass estimation in the loop of weight compensation for the first time. This model has the potential to be used as a cognitive model for justifying how humans are interacting with the environment and how the brain and neuromuscular system are combining the sensory muscle information in order to have a quantitative or a qualitative understanding of the environments and object properties. Some peoples can guess an object mass precisely only by holding it; this model can justify such behaviors. On the other hand, this model can provide a deep sensing method for individuals with hand amputation who still have their sensory neurons.

Acknowledgment

The authors would like to thank the University of Tehran for providing support for this work. Also, we hereby extend our gratitude to Dr. Fariba Bahrami, the head of *Motion Control and Computational Neuroscience Lab*, for providing an EMG device in this research.

References

[1] A. Kapsalyamov, S. Hussain, and P. K. Jamwal, "State-of-the-art assistive powered upper limb exoskeletons for elderly," *IEEE Access*, 2020.

[2] M. A. Gull, S. Bai, and T. Bak, "A review on design of upper limb exoskeletons," *Robotics*, vol. 9, no. 1, p. 16, 2020.

[3] M. R. Islam, B. Brahmi, T. Ahmed, M. Assad-Uz-Zaman, and M. H. Rahman, "Exoskeletons in upper limb rehabilitation: A review to find key challenges to improve functionality," *Control Theory in Biomedical Engineering*, pp. 235–265, 2020.

[4] M. Hosseini, R. Meattini, A. San-Millan, G. Palli, C. Melchiorri, and J. Paik, "A semg-driven soft exosuit based on twisted string actuators for elbow assistive applications," *IEEE Robotics and Automation Letters*, vol. 5, no. 3, pp. 4094–4101, 2020.

[5] B. Treussart, F. Geffard, N. Vignais, and F. Marin, "Controlling an upper-limb exoskeleton by emg signal while carrying unknown load," in *2020 IEEE International Conference on Robotics and Automation (ICRA)*. IEEE, 2020, pp. 9107–9113.

[6] R. Meattini, D. Chiaravalli, G. Palli, and C. Melchiorri, "semg-based human-in-the-loop control of elbow assistive robots for physical tasks and muscle strength training," *IEEE Robotics and Automation Letters*, vol. 5, no. 4, pp. 5795–5802, 2020.

[7] R. Ronsse, N. Vitiello, T. Lenzi, J. Van Den Kieboom, M. C. Carrozza, and A. J. Ijspeert, "Adaptive oscillators with human-in-the-loop: Proof of concept for assistance and rehabilitation," in *2010 3rd IEEE RAS & EMBS International Conference on Biomedical Robotics and Biomechatronics*. IEEE, 2010, pp. 668–674.

[8] J. Zhang, P. Fiers, K. A. Witte, R. W. Jackson, K. L. Poggensee, C. G. Atkeson, and S. H. Collins, "Human-in-the-loop optimization of exoskeleton assistance during walking," *Science*, vol. 356, no. 6344, pp. 1280–1284, 2017.

[9] Y. Ding, M. Kim, S. Kuindersma, and C. J. Walsh, "Human-in-the-loop optimization of hip assistance with a soft exosuit during walking," *Science Robotics*, vol. 3, no. 15, p. eaar5438, 2018.

[10] D. Wei, Z. Li, Q. Wei, H. Su, B. Song, W. He, and J. Li, "Human-in-the-loop control strategy of unilateral exoskeleton robots for gait rehabilitation," *IEEE Transactions on Cognitive and Developmental Systems*, 2019.

[11] F. L. Haufe, P. Wolf, and R. Riener, "Human-in-the-loop optimization of a multi-joint wearable robot for movement assistance," *Proceedings on Automation in Medical Engineering*, vol. 1, no. 1, pp. 023–023, 2020.

[12] Y. Li and S. S. Ge, "Human–robot collaboration based on motion intention estimation," *IEEE/ASME Transactions on Mechatronics*, vol. 19, no. 3, pp. 1007–1014, 2013.

[13] M. Khoramshahi and A. Billard, "A dynamical system approach to task-adaptation in physical human–robot interaction," *Autonomous Robots*, vol. 43, no. 4, pp. 927–946, 2019.

[14] X. Wu, Z. Li, Z. Kan, and H. Gao, "Reference trajectory reshaping optimization and control of robotic exoskeletons for human-robot co-manipulation," *IEEE Transactions on Cybernetics*, 2019.

[15] M. Puchinger, N. B. R. Kurup, T. Keck, J. Zajc, M. F. Russold, and M. Gföhler, "The retrainer light-weight arm exoskeleton: Effect of adjustable gravity compensation on muscle activations and forces," in *2018 7th IEEE International Conference on Biomedical Robotics and Biomechatronics (Biorob)*. IEEE, 2018, pp. 396–401.

[16] P. W. Hill, E. T. Wolbrecht, and J. C. Perry, "Gravity compensation of an exoskeleton joint using constant-force springs," in *2019 IEEE 16th International Conference on Rehabilitation Robotics (ICORR)*. IEEE, 2019, pp. 311–316.

[17] F. Just, Ö. Özen, S. Tortora, V. Klamroth-Marganska, R. Riener, and G. Rauter, "Human arm weight compensation in rehabilitation robotics: efficacy of three distinct methods," *Journal of neuroengineering and rehabilitation*, vol. 17, no. 1, pp. 1–17, 2020.

[18] A.-M. Georgarakis, J. Song, P. Wolf, R. Riener, and M. Xiloyannis, "Control for gravity compensation in tendon-driven upper limb exosuits," in *2020 8th IEEE RAS/EMBS International Conference for Biomedical Robotics and Biomechatronics (BioRob)*. IEEE, pp. 340–345.

[19] D. Park, J. Ortiz, and D. G. Caldwell, "Novel mechanism of upper limb exoskeleton for weight support," in *International Symposium on Wearable Robotics*. Springer, 2018, pp. 510–514.

[20] J. Hull, R. Turner, A. A. Simon, and A. T. Asbeck, "A novel method and exoskeletons for whole-arm gravity compensation," *IEEE Access*, vol. 8, pp. 143 144–143 159, 2020.

[21] M. Asgari, P. T. Hall, B. S. Moore, and D. L. Crouch, "Wearable shoulder exoskeleton with spring-cam mechanism for customizable, nonlinear gravity compensation," in *2020 42nd Annual International Conference of the IEEE Engineering in Medicine & Biology Society (EMBC)*. IEEE, 2020, pp. 4926–4929.

[22] D. A. Winter, "Kinematic and kinetic patterns in human gait: variability and compensating effects," *Human movement science*, vol. 3, no. 1-2, pp. 51–76, 1984.

[23] H. Lee and N. Hogan, "Time-varying ankle mechanical impedance during human locomotion," *IEEE Transactions on Neural Systems and Rehabilitation Engineering*, vol. 23, no. 5, pp. 755–764, 2014.

[24] J. Senefeld, T. Yoon, and S. K. Hunter, "Age differences in dynamic fatigability and variability of arm and leg muscles: Associations with physical function," *Experimental gerontology*, vol. 87, pp. 74–83, 2017.

[25] L. M. Mooney and H. M. Herr, "Biomechanical walking mechanisms underlying the metabolic reduction caused by an autonomous exoskeleton," *Journal of neuroengineering and rehabilitation*, vol. 13, no. 1, p. 4, 2016.

[26] Y. Li, G. Ganesh, N. Jarrassé, S. Haddadin, A. Albu-Schaeffer, and E. Burdet, "Force, impedance, and trajectory learning for contact tooling and haptic identification," *IEEE Transactions on Robotics*, vol. 34, no. 5, pp. 1170–1182, 2018.

[27] D. P. Ferris, G. S. Sawicki, and M. A. Daley, "A physiologist's perspective on robotic exoskeletons for human locomotion," *International Journal of Humanoid Robotics*, vol. 4, no. 03, pp. 507–528, 2007.

[28] T. J. Roberts and A. M. Gabaldón, "Interpreting muscle function from emg: lessons learned from direct measurements of muscle force," *Integrative and comparative biology*, vol. 48, no. 2, pp. 312–320, 2008.

[29] M. Cifrek, V. Medved, S. Tonković, and S. Ostojić, "Surface emg based muscle fatigue evaluation in biomechanics," *Clinical biomechanics*, vol. 24, no. 4, pp. 327–340, 2009.

[30] K. Kiguchi and Y. Hayashi, "An emg-based control for an upper-limb power-assist exoskeleton robot," *IEEE Transactions on Systems, Man, and Cybernetics, Part B (Cybernetics)*, vol. 42, no. 4, pp. 1064–1071, 2012.

[31] R. A. R. C. Gopura, K. Kiguchi, and Y. Li, "Sueful-7: A 7dof upper-limb exoskeleton robot with muscle-model-oriented emg-based control," in *2009 IEEE/RSJ International Conference on Intelligent Robots and Systems*. IEEE, 2009, pp. 1126–1131.

[32] L. Peternel, T. Noda, T. Petrič, A. Ude, J. Morimoto, and J. Babič, "Adaptive control of exoskeleton robots for periodic assistive behaviours based on emg feedback minimisation," *PloS one*, vol. 11, no. 2, p. e0148942, 2016.

[33] S. Mghames, M. Laghi, C. Della Santina, M. Garabini, M. Catalano, G. Grioli, and A. Bicchi, "Design, control and validation of the variable stiffness exoskeleton flexo," in *Rehabilitation Robotics (ICORR), 2017 International Conference on*. IEEE, 2017, pp. 539–546.

[34] R. Nasiri, M. Rayati, and M. N. Ahmadabadi, "Feedback from monoarticular muscles is sufficient for exoskeleton torque adaptation," *IEEE Transactions on Neural Systems and Rehabilitation Engineering*, vol. 27, no. 10, pp. 2097–2106, 2019.

[35] A. Erdemir, S. McLean, W. Herzog, and A. J. van den Bogert, "Model-based estimation of muscle forces exerted during movements," *Clinical biomechanics*, vol. 22, no. 2, pp. 131–154, 2007.

[36] J. Bobet and R. Norman, "Least-squares identification of the dynamic relation between the electromyogram and joint moment," *Journal of biomechanics*, vol. 23, no. 12, p. 1275—1276, 1990.

[37] H. K. Khalil, *Nonlinear systems*. Prentice hall Upper Saddle River, 2002.

[38] S. L. Delp, F. C. Anderson, A. S. Arnold, P. Loan, A. Habib, C. T. John, E. Guendelman, and D. G. Thelen, "Opensim: Open-source software to create and analyze dynamic simulations of movement," *IEEE Transactions on Biomedical Engineering*, vol. 54, no. 11, pp. 1940–1950, 2007.

[39] K. R Saul, X. Hu, C. M. Goehler, M. E. Vidt, M. Daly, A. Velisar, and W. M. Murray, "Benchmarking of dynamic simulation predictions in two software platforms using an upper limb musculoskeletal model," *Computer methods in biomechanics and biomedical engineering*, vol. 18, pp. 1445–1458, 2015.

[40] K. RS Holzbaur, W. M Murray, and S. L. Delp, "A model of the upper extremity for simulating musculoskeletal surgery and analyzing neuromuscular control," *Annals of biomedical engineering*, vol. 33, pp. 829–840, 2005.

[41] F. Zajac, "Muscle and tendon: properties, models, scaling, and application to biomechanics and motor control," *Crit. Rev. Biomed. Eng.*, vol. 17, no. 4, pp. 359–411, 1989.
[42] MATLAB, *version 9.8 (R2020a)*. Natick, Massachusetts: The MathWorks Inc., 2020.
[43] D. G. Thelen and F. C. Anderson, "Using computed muscle control to generate forward dynamic simulations of human walking from experimental data," *J. Biomech.*, vol. 39, no. 6, pp. 1107–1115, 2006.
[44] A. d'Avella, A. Portone, L. Fernandez, and F. Lacquaniti, "Control of fast-reaching movements by muscle synergy combinations," *Journal of Neuroscience*, vol. 26, no. 30, pp. 7791–7810, 2006.